AIP Advances

Prospective for graphene based thermal mid-infrared light emitting devices

L. M. Lawton, N. H. Mahlmeister, I. J. Luxmoore, and G. R. Nash

Citation: AIP Advances **4**, 087139 (2014); doi: 10.1063/1.4894449
View online: http://dx.doi.org/10.1063/1.4894449
View Table of Contents: http://scitation.aip.org/content/aip/journal/adva/4/8?ver=pdfcov
Published by the AIP Publishing

AIP ADVANCES **4**, 087139 (2014)

Prospective for graphene based thermal mid-infrared light emitting devices

L. M. Lawton, N. H. Mahlmeister, I. J. Luxmoore, and G. R. Nash[a]
College of Engineering, Mathematics and Physical Sciences, University of Exeter, Exeter, EX4 4QF, U.K.

(Received 20 May 2014; accepted 20 August 2014; published online 29 August 2014)

We have investigated the spatial and spectral characteristics of mid-infrared thermal emission from large area Chemical Vapor Deposition (CVD) graphene, transferred onto SiO_2/Si, and show that the emission is broadly that of a grey-body emitter, with emissivity values of approximately 2% and 6% for mono- and multilayer graphene. For the currents used, which could be sustained for over one hundred hours, the emission peaked at a wavelength of around 4 μm and covered the characteristic absorption of many important gases. A measurable modulation of thermal emission was obtained even when the drive current was modulated at frequencies up to 100 kHz. [http://dx.doi.org/10.1063/1.4894449]

One of the many distinguishing features of graphene is its ability to sustain extremely large current densities of, for example, approximately 10^9 A/cm^2 in nanoribbons[1] and 10^7 A/cm^2 in micron sized wires fabricated from graphene grown by chemical vapor deposition (CVD),[2] which compares to the values of ~100 A/cm^2 in a conventional 100W tungsten filament light bulb. Although this makes it attractive for potential use as an incandescent source,[3] thermal emission from graphene has primarily been used over the last few years as a means of probing the electronic structure of graphene transistor devices under bias.[4–7] However, there is a continuing need for the development of new infrared sources to enable low cost, intrinsically safe, portable infrared gas sensors for applications such as mine safety. Most existing infrared (IR) sensors use conventional incandescent sources which have several shortcomings including slow response time, limited wavelength range (due to the glass envelope of the source), limited lifetimes due to the fragility of the source, relatively high power consumption, and a requirement for explosion proof housings to prevent the source from igniting flammable gases that may be present. These disadvantages have proved an impediment to infrared sensors replacing existing sensor technologies in the installed base of sensors (such as electrochemical cells). An alternative to conventional incandescent sources are microelectromechanical systems (MEMS) silicon thermal emitters,[9] which arose from work developing bolometer detectors. However, these components still have a relatively slow response time (maximum modulation frequencies of ~100Hz). Semiconductor light emitting diodes (LEDs)[10] offer advantages in terms of modulation speed, but it is only in the last decade or so that room temperature operation at IR wavelengths has been demonstrated. These LEDs also suffer from a poor radiative efficiency (the amount of electrical power converted into optical power) which is partly limited by non-radiative Auger recombination.[11] This is an intrinsic process which depends on the carrier concentration and therefore becomes increasingly important as the semiconductor bandgap is narrowed to obtain emission in the mid-infrared. In combination with the relatively high refractive index of the narrow band semiconductors used to fabricate these LEDs, which limits the number of generated photons escaping the device,[12] the overall efficiency of mid-infrared LEDs is relatively low. For example, the room temperature wall-plug efficiency (WPE) of the $Al_xIn_{1-x}Sb$

[a]Correspondence: g.r.nash@exeter.ac.uk

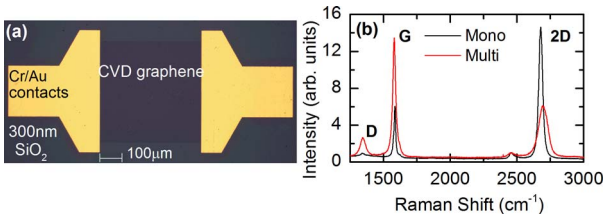

FIG. 1. (a) Image of a typical device; CVD monolayer graphene 0.5 mm × 0.6 mm. (b) Average Raman spectrum recorded from the monolayer (black) and thick multilayer (red) graphene.

based LEDs described by Nash *et al*[12] was approximately 0.02%. A much higher WPE of 0.15% has recently been reported in interband cascade light emitting devices with peak emission at 3.3 μm,[13] but this is still much lower than in LEDs operating at shorter wavelengths.

In this paper, we investigate the thermal emission from large area graphene (mono- and multi-layer) and demonstrate that its extraordinary electrical conductivity, coupled with its low thermal mass (approximately three orders of magnitude smaller even than a typical silicon cantilevers), offers the prospect of developing a new generation of high frequency infrared sources.

Devices were fabricated from pre-transferred monolayer and multilayer graphene (obtained from Graphene Square and Graphene Supermarket) on 300 nm thick SiO_2, with a highly doped Si substrate. Large 0.5 mm × 0.6 mm areas of graphene were defined using electron beam lithography and an O_2/Ar reactive ion etch, and Cr/Au (7/70 nm) source and drain contacts, 0.6 mm long and 0.2 mm wide, were deposited on top of the graphene using thermal evaporation, leaving an exposed graphene area of 0.5 mm × 0.5 mm. A microscope image of the monolayer device is shown in Fig. 1(a). After deposition of the contacts, multiple Raman spectra were taken using a 100 mW 532 nm continuous wave laser, from a number of different points, to confirm the nature and uniformity of the graphene, with the average of the measured spectra shown in Fig. 1(b). A closer examination of the 2D peaks confirms the symmetrical characteristic associated with monolayer graphene,[14,15] and implies that the multilayer graphene contains 3–6 layers.[16]

The devices were mounted on ceramic chip holders and placed in a vacuum chamber, with a CaF_2 window for optical access, which was evacuated to $\sim 10^{-5}$mbar. Two terminal current-voltage measurements were made at room temperature, using a pulsed DC current source. Resistance values at a low source drain current of 1mA of 1750 Ω/□ and 1300 Ω/□ were calculated for the monolayer and multilayer devices respectively (the resistances due to contacts and measurement leads were assumed to be negligible). These values are typical of those obtained from CVD graphene.[17] Measurements of the resistance immediately after optical characterisation had been performed, during which large currents were used and the devices became hot, yielded a lower resistance of 1560 Ω/□ in the monolayer graphene device and higher a resistance 1540 Ω/□ in the multilayer device. Such resistance quenching with increasing temperature has previously been observed in both single, and bilayer graphene interconnects[18] and is thought to be due to the thermal generation of electron-hole pairs and carrier scattering by acoustic phonons. The higher resistance observed in the multilayer sample with increasing temperature is as one would expect for a conventional semi-metal.

Spectral and thermal emission mapping measurements were performed using a Keithley 6221 current source with devices driven typically by a 1 kHz square waveform (50% duty cycle), at peak injection currents of tens of milliamps. For mapping measurements, the thermal emission was collected using a 15x reflecting objective lens (Numerical aperture = 0.28) and focused, using a CaF_2 lens, onto a liquid nitrogen cooled HgCdTe detector, with a 2–12 μm response. The reflecting objective, CaF_2 lens and detector were mounted on a xy-stage and the spatial variation of the thermal emission was measured by scanning the microscope system over the device. The signal from the detector was amplified by a low noise preamplifier, and passed to a lock-in amplifier for phase sensitive measurement. The measured spatial variation of the thermal emission from the mono- and multi-layer devices for peak currents of 44mA and 52mA, and under zero gate bias, respectively are shown in Figures 2(a) and 2(b), respectively. The emission from the monolayer device is dominated by a single large hot-spot, similar to that previously observed in micron-scale exfoliated graphene

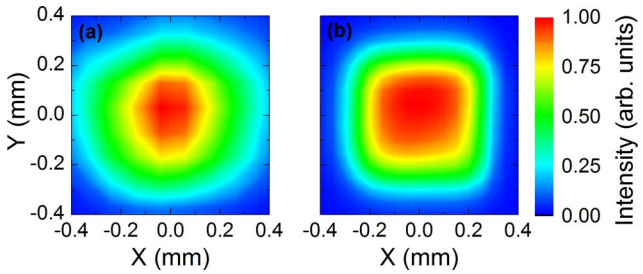

FIG. 2. Thermal emission mapped from large area (a) monolayer device with peak injection current of 44mA (b) multilayer device with peak injection current of 52 mA.

devices,[3–7] and also in large area CVD devices,[8] where the thermal emission is dominated by Joule heating governed by the charge distribution along the channel. In this case given the symmetrical nature and scaling of the emission we estimate the hotspot to be approximately half-way between the source and the drain contacts. Although a relatively high gate leakage in this particularly device prevented the position of the hot-spot being moved as a function of gate bias, corresponding to a movement of the Dirac point, we were able to move the hotspot on other similar large area devices. This confirms that these large area devices retain the characteristic nature of graphene.[8] In contrast to that obtained from the monolayer, the emission from the multilayer device occurs more uniformly over the whole exposed area, consistent with a uniform channel resistance. This behavior is typical of a relatively long conventional filament supported by two colder supports, suggesting that for these purposes the multilayer device can be thought of this way. The magnitude of the emission at each 'hot-spot' demonstrates an approximate dependence on the current squared, indicative of a Joule heating mechanism. Finally, in both cases the thermal emission extends approximately only over the area of the graphene. As the magnitude of the signal corresponds to the difference between the thermal emission when the current is on and off, this suggests that it is only the temperature of the graphene which changes on the timescales defined by the current pulses in the timescales defined by the length and period of the current pulses.

Emission spectra were collected using a Jobin-Yvon iHR550 grating spectrometer, together with a cooled HgCdTe detector, with a 2–12 μm response. Devices were driven with 50% duty cycle 1 kHz square waves (pulse length $\sim$ 0.5 ms), with peak currents of 44mA and 60mA for the monolayer and multilayer devices respectively, in order to give approximately equal power densities. The signal from the detector was again amplified by a low noise preamplifier, and passed to a lock-in amplifier for phase sensitive measurement. Spectra were collected over the 2 to 10 μm range by combining data from that obtained using two different diffraction gratings: a 4 μm blazed (300 lines per mm) grating for the 2–6 μm region, and an 8 μm blazed (150 lines per mm) for the 4 to 10 μm range. In the Fig. 3(a) the raw emission spectra in the 2–6 μm range are shown for the two devices, together with that obtained from a blackbody calibration source set to a temperature of 673 K. The shape of the emission spectra is very similar in all cases, with a peak in emission at approximately 4 μm, suggesting that emission from the graphene devices corresponds broadly to that of a grey-body. The large dip in emission at approximately 4.2 μm is due to CO_2 absorption, whereas absorption by water will affect the spectra at wavelengths smaller than $\sim$3 μm, and greater than $\sim$5 μm. The maximum intensity of the emission from the blackbody source is approximately 32 times greater than that obtained from the multilayer device, which is in turn approximately three times that of the monolayer emission. Due to the similarity of the emission spectra, and taking the emissivity of the blackbody calibrator to be 0.95, the difference in measured intensities allows an estimate to be made of the emissivity of the monolayer and multilayer graphene, yielding values of approximately 2% and 6% respectively. This is in good agreement with the measured absorbance of $\alpha = 2.3\%$ for monolayer graphene[19,20] and with the emissivity value of $1.6 \pm 0.8\%$ extracted from thermal emission measurements on monolayer graphene by Freitag *et al.*[6] As the emissivity is expected to increase linearly with the number of layers in a multilayer device, this also suggests that the thick multi-layer device consists of approximately three layers.

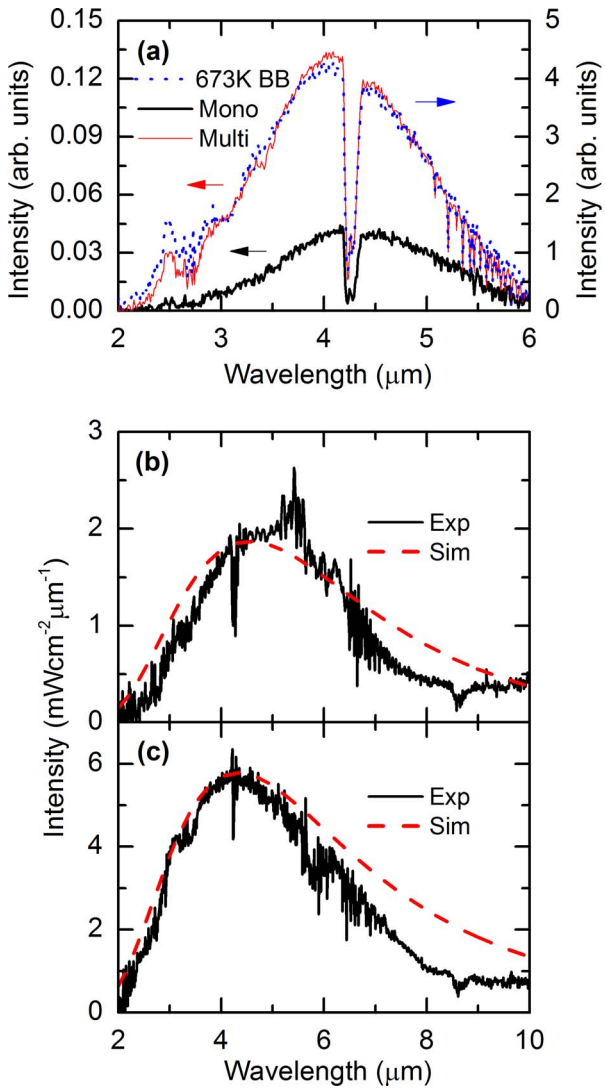

FIG. 3. (a) Measured raw emission spectra from monolayer (black) and multilayer (red) graphene, and 673 K blackbody calibration source (green). Corrected emission spectra from (b) monolayer (c) multilayer devices, together with simulated spectra (dashed).

To correct for the efficiency of the spectrometer grating, the detector response and absorption by CO_2 and water in the atmosphere, the spectral measurements were calibrated using the 673 K blackbody source, and calibrated emission spectra are shown in Figs. 3(b) and 3(c) for the monolayer and multilayer devices respectively (note that Savitzky-Golay smoothing was applied to the measured data). At the drive currents used, the emission covers the part of the spectrum where many important gases, including carbon dioxide and nitric oxide, have their characteristic absorption. The total integrated emission was 7.7 mW/cm^2 and 22 mW/cm^2 for the mono-layer and multi-layer samples respectively, yielding a maximum wall plug efficiency of approximately 0.001%. However, it's likely that this efficiency can be improved simply by optimizing the number of graphene layers and the geometry of the devices.

Calculated spectra are also shown in Figs. 3(b) and 3(c). As the signal measured on the lock-in amplifier again corresponds to the difference between the thermal emission when the current is on and off, the calculated spectra were obtained by calculating the difference between two grey-body curves, one corresponding to emission from the hot graphene when the current is on, and the second corresponding to the cooler background temperature of the underlying silicon dioxide/silicon when

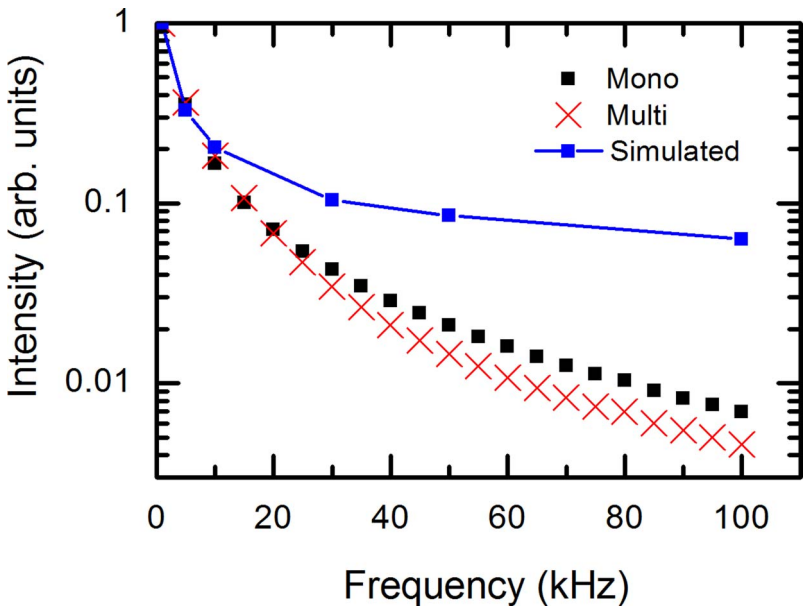

FIG. 4. Measured and simulated values of the emission intensity as a function of the frequency of the applied current (symbols), where the values have been normalized to those at 1 kHz. The line is a guide for the eye only.

the current is off, consistent with the mapping measurements. Values of 2%, 6% and 6% were taken for the emissivity of the monolayer, multi-layer, and silicon respectively,[21] yielding temperatures of the graphene and background silicon chip of 600 K and 350 K for the monolayer, and 620 K and 480 K for the multilayer devices (as the currents are applied for many hours during measurements, the silicon substrate reaches an equilibrium background temperature). Note that we are assuming that the graphene emitting area reaches equilibrium with the underlying substrate when the current is off, but further work would be needed to confirm this. Over much of the wavelength range there is good agreement between the measured data and calculations, which are relatively simple and not designed to be a fit to the data, confirming that the emission from both devices is primarily that of a grey-body (it is unclear why the calculations and measurements agree less well over the 7–10 μm region).

To gain insight into the modulation frequencies at which a graphene based emitter could be driven; the emission from the devices was measured as a function of the drive current frequency, as shown in Figure 4 (where the measured signals have been normalized to that obtained at 1 kHz). Note that in previous studies[4–6] either continuous currents, or pulsed currents at a fixed frequency, have been used to heat the graphene. In our frequency measurements, the emission was measured via the spectrometer, but using a mirror rather than a diffraction grating. As before, the signal measured on the lock-in amplifier again corresponds to the difference between the thermal emission when the current is on and off. For both devices, there is still a measurable signal up to 100 kHz, corresponding to a pulse width of 5μs, which is the frequency limit of the current source. At frequencies above 20 kHz, the rate of decrease of the intensity is smaller for the monolayer sample compared to that of the multilayer sample, which could perhaps reflect the difference in thermal mass between the two. This switching is much faster than typical MEMS based emitters.[22] To investigate the mechanisms limiting the speed of modulation in these devices, the effect of increasing the modulation frequency of the applied current was modeled using COMSOL finite element software. A 2D joule heating model of the multilayer device was constructed, with gold contacts connecting a thin (5 nm) graphite layer sitting on top of 300 nm of SiO_2 and a 500 μm of doped Si. A current of 0.6A was applied as a square function (50% duty cycle), to give a current density similar to that in the real devices, at frequencies ranging from 1 kHz to 100 kHz. In this case, we have assumed that the base of the silicon substrate remains at room temperature, that there is no convection or radiation (due to the very low emissivity), that there is no thermal barrier between the graphite and the SiO_2,

and that the material properties are constant and not a function of temperature or pressure. Material properties were also assumed to be isotropic except for thermal conductivity, which was assumed to be anisotropic with an in-plane thermal conductivity equal to that of graphene[23] and an out-of-plane thermal conductivity equal to that of pyrolytic graphite along the c-axis.[24] Peak temperatures of the graphite layer during the 'on' and 'off' state of the current were calculated (688 K and 382 K respectively at 1 KHz) as a function of frequency, and these values were then used to first calculate the emitted spectra, and then the expected measured intensity (taking into account the detector response, and also that the measured signal is the difference between the "on" and "off" states). The calculations show that the peak emission of the emitting area shifts from 4.2 μm at 1 kHz to 5.9 μm at 10 kHz and 7.3 μm at 100 kHz. At low frequencies, there is good agreement between the calculated and measured change in intensity, the steep initial decrease reflecting the fact that a small decrease in the temperature of the emitting area (which in the simulations is 489 K at 10 KHz) leads to a large decrease in the emission due to the latter's dependence on the temperature to the power four. At high frequencies, the calculated values show a much smaller decrease than those measured. It is unclear at this stage whether this difference is due to the inherent response of our measurement system, or whether some of the assumptions in the modeling (e.g. that there is no thermal barrier between the graphite and SiO_2) and further work is underway to investigate this. However, the low thermal time constant of graphene transistors calculated previously[25] suggests it will be possible to obtain higher intensities at high frequencies through electrical and thermal management.

In conclusion, we have investigated the characteristics of thermal emission from large area graphene devices and have shown that emission is broadly that of a grey-body emitter, with emissivity values of approximately 2% and 6% for mono- and multi-layer graphene. For the currents used, which could be sustained by the devices for over one hundred hours, the emission peaked at a wavelength of around 4 μm and covered the characteristic absorption of many important gases. A measurable thermal emission was obtained even when the drive current was modulated at frequencies up to 100 kHz. In combination, these demonstrate the feasibility of developing a graphene based mid-infrared light emitting device, which could be more cost effective and sustainable to manufacture than either silicon MEMs or compound semiconductor based alternatives. Further work is now underway to investigate methods of increasing the potential modulation speed and of increasing the emissivity of the emitting area.

ACKNOWLEDGMENTS

This work has been undertaken as part of an EPSRC Fellowship in Manufacturing (GRN), and of the project "GOSFEL", which has received funding from the European Union for this research. The authors would also like to thank Timothy Poole and Choon How Gan for useful discussions.

[1] R. Murali, K. Brenner, Y. X. Yang, T. Beck, and J. D. Meindl, Electron Device Lett. **30**, 611 (2009).
[2] K-Jae Lee, A. P. Chandrakasan, Fellow, and J. Kong, Electron Device Lett. **33**, 557 (2011).
[3] See, for example, D. Yu and L. Dai, Appl. Phys. Lett. **96**, 143107 (2010).
[4] M. Bae, Z. Ong, D. Estrada, and E. Pop, Nano Lett. **10**, 4787 (2010).
[5] M. H. Bae, S. Islam, V. E. Dorgan, and E. Pop, ACS Nano **5**, 7936 (2011).
[6] M. Freitag, H.-Y. Chiu, M. Steiner, V. Perebeinos, and P. Avouris, Nature Nanotech. **5**, 497 (2010).
[7] K. L. Grosse, M. H. Bae, F. Lian, E. Pop, and W. P. King, Nature Nanotech. **6**, 287 (2011).
[8] I. J. Luxmoore, C. Adlem, T. Poole, L. M. Lawton, N. H. Mahlmeister, and G. R. Nash, Appl. Phys. Lett. **103**, 131906 (2013).
[9] See, for example, M. Parameswaran, A. M. Robinson, D. L. Blackburn, M. Gaitan, and J. Geist, IEEE Electron Device Lett. **12**, 57 (1991).
[10] See, for example, N. V. Zotova, N. D. Il'inskaya, S. A. Karandashev, B. A. Matveev, M. A. Remennyi, and N. M. Stus', Semiconductors **40**, 697 (2006); M. K. Haigh, G. R. Nash, S. J. Smith, L. Buckle, M. T. Emeny, and T. Ashley, Appl. Phys. Lett. **90**, 231116 (2007); G. R. Nash, H. L. Forman, S. J. Smith, P. B. Robinson, L. Buckle, S. D. Coomber, M. T. Emeny, N. T. Gordon and T. Ashley, IEEE Sensors Journal **9**, 1240 (2009) and K. J. Cheetham, A. Krier, I. P. Marko, A. Aldukhayel, and S. J. Sweeney, Appl. Phys. Lett. **99**, 141110 (2011).
[11] B. I. Mirza, G. R. Nash, S. J. Smith, L. Buckle, S. D. Coomber, M. T. Emeny, and T. Ashley, J. Appl. Phys. **104**, 063113 (2008).
[12] I. J. Buss, M. J. Cryan, C. J. Railton, I. J. Craddock, G. R. Nash, J. G. Rarity, J. Opt. Soc. Am. B. **25**, 810 (2008).
[13] J. Abell, C. S. Kim, W. W. Bewley, C. D. Merritt, C. L. Canedy, I. Vurgaftman, J. R. Meyer and M. Kim, Appl. Phys. Lett. **104**, 261103 (2014).
[14] A. Reina, X. Jia, J. Ho, D. Nezich, H. Son, V. Bulovic, M. S. Dresselhaus, and J. Kong, Nano Lett. **9**, 30 (2009).

[15] A. C. Ferrari, J. C. Meyer, V. Scardaci, C. Casiraghi, M. Lazzeri, F. Mauri, S. Piscanec, D. Jiang, K. S. Novoselov, S. Roth, and A. K. Geim, Phys. Rev. Lett. 187401 (2006).
[16] D. Graf, F. Molitor, K. Ensslin, C. Stampfer, A. Jungen, C. Hierold, and L. Wirtz, Nano Lett. **7**, 238 (2007).
[17] X. Li, Y. Zhu, W. Cai, M. Borysiak, B. Han, D. Chen, R. D. Piner, L. Colombo, and R. S. Ruoff, Nano Lett. **9**, 4359 (2009).
[18] Q. Shao, G. Liu, D. Teweldebrhan, and A. A. Balandin, Appl. Phys. Lett. **92**, 202108 (2008).
[19] R. R. Nair, P. Blake, A. N. Grigorenko, K. S. Novoselov, T. J. Booth, T. Stauber, N. M. R. Peres, and A. K. Geim, Science **320**, 1308 (2008).
[20] K. F. Mak, M. Y. Sfeir, Y. Wu, C. Hung Lui, J. A. Misewich, and T. F. Heinz, Phys. Rev. Lett. **101**, 196405 (2008).
[21] N. M. Ravindra, B. Sopori, O. H. Gokce, X. Cheng, A. Shenoy, L. Jin, S. Abedrabbo, W. Chen and Y. Zhang, International Journal of Thermophysics **22**, 1593, (2001).
[22] H. Sana, X. Chena, M. Chenga, and F. Lia, Proc. SPIE **6836**, 68360N (2007).
[23] A. N. Sidorov, D. K. Benjamin, and C. Foy, Appl. Phys. Lett. **103**, 243103 (2013).
[24] E. Pop, V. Varshney, and A. K. Roy, MRS Bulletin **37**, 1273 (2012).
[25] S. Islam, Z. Li, V. E. Dorgan, M.-H. Bae, and E. Pop, IEEE Electron Device Lett. **34**, 166 (2013).